Two-nucleon $^1S_0$ amplitude zero in chiral effective field theory

M. Sánchez Sánchez,[1] C.-J. Yang,[1] Bingwei Long (龙炳蔚),[2,*] and U. van Kolck[1,3]

[1]*Institut de Physique Nucléaire, CNRS/IN2P3, Univ. Paris-Sud, Université Paris-Saclay, 91406 Orsay, France*

[2]*Center for Theoretical Physics, Department of Physics, Sichuan University, 29 Wang-Jiang Road, Chengdu, Sichuan 610064, China*

[3]*Department of Physics, University of Arizona, Tucson, Arizona 85721, USA*

(Received 28 April 2017; published 5 February 2018)

We present a new rearrangement of short-range interactions in the $^1S_0$ nucleon-nucleon channel within chiral effective field theory. This is intended to address the slow convergence of Weinberg's scheme, which we attribute to its failure to reproduce the amplitude zero (scattering momentum $\simeq 340$ MeV) at leading order. After the power counting scheme is modified to accommodate the zero at leading order, it includes subleading corrections perturbatively in a way that is consistent with renormalization-group invariance. Systematic improvement is shown at next-to-leading order, and we obtain results that fit empirical phase shifts remarkably well all the way up to the pion-production threshold. An approach in which pions have been integrated out is included, which allows us to derive analytic results that also fit phenomenology surprisingly well.

DOI: 10.1103/PhysRevC.97.024001

I. INTRODUCTION

The nuclear effective field theory (EFT) program [1,2] conceives nuclear physics as the renormalization-group (RG) evolution of quantum chromodynamics (QCD) at low energies, formulated in terms of effective degrees of freedom (nucleons, pions, etc.). The link with QCD written in terms of more fundamental objects (quarks and gluons) is ensured by imposing QCD symmetries (particularly approximate chiral symmetry) as the only constraints on the otherwise most general EFT Lagrangian. Power counting (PC) rules tell which terms in this Lagrangian (of an infinite number) should be taken into account when computing observables at a given order in an expansion in powers of the small parameter $Q/M_{\rm hi}$, where Q is the characteristic external momentum of a process and $M_{\rm hi} \lesssim M_{\rm QCD} \sim 1$ GeV is the EFT breakdown scale. Thanks to the recent development of *ab initio* methods, which bridge the gap between nuclear forces and currents on one hand and nuclear structure and reactions on the other, chiral EFT (χEFT) [1–3] is now better exploited than ever. However, problems remain in the formulation of this EFT, some of which we address here in the simplest, yet surprisingly challenging, two-nucleon (NN) channel—the spin-singlet, isospin-triplet S wave, $^1S_0$.

The initial applications of χEFT followed a scheme suggested by Weinberg [4,5] and Rho [6], where a PC dictated by naive dimensional analysis (NDA) [7,8] was assumed to apply to the nuclear potential and currents. The truncated potential is inserted into a dynamical equation—Lippmann-Schwinger (LS), Schrödinger, or one of their variants for the many-body system—from whose exact solution nuclear wave functions are obtained. Averages of the appropriate, truncated currents give rise to scattering amplitudes when the system is probed by external particles such as photons or pions. To deal with the singular nature of the potential and currents, an arbitrary regularization procedure must be introduced. Unfortunately, already at leading order (LO) NDA does not yield all the short-range interactions necessary for the NN amplitude to be approximately independent of the regulator choice [9–11]. Similar issues appear at higher orders [12–14] and also affect electromagnetic currents [15]. Given that nonperturbative renormalization can differ significantly from the perturbative renormalization used to infer NDA, it is perhaps unsurprising that a scheme based solely on NDA fails to produce nuclear amplitudes consistent with RG invariance.

This problem appears even in NN scattering in the $^1S_0$ channel, where one-pion exchange (OPE) has a delta-function singularity in coordinate space. While NDA prescribes that the contact term, which supplements OPE in the LO potential, is chiral-invariant, renormalization demands that a chiral-symmetry-breaking short-range interaction also be present [9]. According to NDA, such a chiral-breaking interaction, being proportional to two powers of the pion mass, should not appear before two more orders (next-to-next-to-leading order or N^{2}LO) in the $Q/M_{\rm hi}$ expansion. This "chiral inconsistency" motivated Kaplan, Savage, and Wise [16,17] to propose a PC where pion exchanges are treated as perturbative corrections starting at next-to-leading order (NLO).[1] However, higher-order calculations soon made clear that such an approach is

[1]Note that throughout the present paper NLO refers to subleading contributions of $\mathcal{O}(Q/M_{\rm hi})$, N^{2}LO to $\mathcal{O}(Q^2/M_{\rm hi}^2)$, and so on. This notation differs from that used by some authors (see, e.g., Ref. [3]) who work under the assumptions of NDA—in which case $\mathcal{O}(Q/M_{\rm hi})$ contributions to the parity-conserving NN potential vanish [18,19]—and refer to contributions of $\mathcal{O}(Q^2/M_{\rm hi}^2)$ as "NLO." When RG invariance is imposed, however, $\mathcal{O}(Q/M_{\rm hi})$ contributions do not vanish even for parity-conserving processes.

*bingwei@scu.edu.cn

not valid at low momenta in certain partial waves [20]. The alternative is to treat OPE as LO only in the lower waves [10,21–27], where suppression by the centrifugal barrier is not effective. The angular-momentum suppression factor has been studied recently in peripheral spin-singlet channels [28].

The $^1S_0$ partial wave was excluded from the analysis in Ref. [28] because this particular channel presents, in addition to the above renormalization issue, other features that are not completely understood. The situation has not improved greatly since the late 1990s, despite considerable effort [13,26,29–57]. Some of this work has been reviewed recently in Refs. [58,59].

A unique feature of this channel, which was recognized early, is fine-tuning in the form of a very shallow virtual bound state. OPE is characterized by two scales, its inverse range given by the pion mass m_π and its inverse strength given by $M_{NN} \equiv 16\pi f_\pi^2/(g_A^2 m_N) = \mathcal{O}(f_\pi)$, where $m_N = \mathcal{O}(M_{\rm QCD})$ is the nucleon mass, $f_\pi = \mathcal{O}(M_{\rm QCD}/(4\pi))$ is the pion decay constant, and $g_A = \mathcal{O}(1)$ is the axial-vector coupling constant. At the physical pion mass $m_\pi \approx 140$ MeV, the virtual state's binding momentum $\aleph \sim 10$ MeV is much smaller than the pion scales and can only be reproduced at LO through a fine-tuning of the short-range interaction. Physics of this state can be described simply by another successful, renormalizable EFT, pionless (or contact) EFT ($\not\pi$EFT). In the very low energy regime of nuclear physics, $Q \ll m_\pi$, pion exchange cannot be resolved, the EFT Lagrangian contains only contact interactions, and the two-body amplitude reduces [16,17,60,61] to the effective range expansion (ERE). To simultaneously capture physics at $Q \sim m_\pi$, however, pion exchange needs to be retained. The perturbative expansion in Q/M_{NN} prescribed by Refs. [16,17] converges very slowly, if at all, in the low-energy region [38], which leads to the identification of M_{NN} as a low-energy scale $M_{\rm lo}$, just as suggested by NDA.

Yet it is disturbing that the NDA-prescribed LO potential produces $^1S_0$ phase shifts that show large discrepancies with the Nijmegen partial-wave analysis (PWA) [62,63] even at moderate scattering energies. In Ref. [26] it was shown that—again at variance with NDA—the first correction in this channel appears already at NLO in the form of a contact interaction with two derivatives. Still, only about half of the energy dependence of the amplitude near threshold is accounted for at LO, so Ref. [54] went a step further by suggesting the promotion to LO of an energy-dependent short-range interaction that reproduces the effective range—a generalization of the same suggestion for $\not\pi$EFT [64]. Even this promotion leaves significant room for improvement when compared to the Nijmegen PWA. In particular, the empirical $^1S_0$ phase shift, thus the amplitude, vanishes at a center-of-mass momentum $k = k_0 \simeq 340$ MeV. Since k_0 is significantly below the expected breakdown scale $M_{\rm QCD}$, we should consider it as a soft scale where the EFT converges. In contrast, we find that the LO phase shift of Ref. [54] is around 25° at $k = k_0$ and does not vanish until k reaches a few GeV. Since higher orders need to overcome LO, convergence at momenta $k \sim k_0$ will be at best very slow. This can only be remedied if LO contains the amplitude zero. As pointed out in Ref. [61], a low-energy zero requires a different kind of fine-tuning than the one that gives rise to a shallow bound state. When the zero appears at very low energies, a contact EFT can be devised (the "other unnatural EFT" of Ref. [61]) which gives rise to a perturbative expansion of the amplitude. Such an expansion around $k = k_0$ in the presence of pions was developed in Ref. [37].

Here we propose a rearrangement of the short-range part of χEFT that leads to the existence of the amplitude zero at LO, in addition to the shallow virtual state. The PC of Ref. [61] is generalized with the purpose of including the nonperturbative region that contains the virtual state. This is patterned on an idea originally developed for doublet neutron-deuteron (nd) scattering at very low energies [65], where the amplitude has a zero at small imaginary momentum, in addition to a shallow virtual state. We develop an expansion in $Q/M_{\rm hi}$ for $Q \sim M_{\rm lo}$, which gives a renormalizable amplitude order by order. Following a successful approach to $\not\pi$EFT [66], the virtual state is assumed to be located right at threshold at LO and is moved to a binding momentum $\sim M_{\rm lo}^2/M_{\rm hi}$ at NLO. We calculate NLO corrections and show a systematic improvement in the description of the phase shift. We also show results where the binding momentum is taken as an LO fitting parameter.

A challenging feature of χEFT is that it usually does not yield analytical expressions for amplitudes. In order to facilitate an understanding of the properties of the NN amplitude, we also consider a version of our PC for the theory without explicit pions, where we retain $k_0 \sim M_{\rm lo}$ but artificially take $M_{NN} \to \infty$. To our surprise, even though $k_0 > m_\pi$, this hypothetical version of $\not\pi$EFT also produces a good description of the empirical phase shifts.

Our approach is in line with Refs. [35,50], which argued that short-range forces in the spin-singlet S wave must produce rapid energy dependence. It is a systematic extension of the potential proposed in Ref. [29], and it resembles the unitarized approach of Ref. [37]. More generally, it can be seen as the EFT realization of Castillejo-Dalitz-Dyson (CDD) poles [67] in S-matrix theory. Traditional S-matrix tools, such as the N/D method, have recently received renewed attention in the NN system (e.g., Ref. [68]). The D function is determined modulo the addition of CDD poles, which result in zeros of the scattering amplitude. In particular, the momentum k_0 may be identified with the position of a CDD pole in the $^1S_0$ channel [69]. An EFT provides a systematic description of the two-body CDD pole, which can be naturally extended to more-body systems.

This article is structured as follows. In Sec. II we present an initial approach ("warm-up") to the problem on the basis of a modified organization of $\not\pi$EFT up to NLO. The proposed PC is discussed in detail, and RG invariance is demonstrated explicitly. In Sec. III we bring OPE into LO; also, we compare with the results [63] of the high-quality Nijm93 potential [70] before and after the inclusion of the NLO potential in this χEFT. Conclusions and outlook are presented in Sec. IV.

II. PIONLESS THEORY

Our first approach to the problem will omit explicit pion exchange (and also electromagnetic interactions, which are small for $k \gtrsim 10$ MeV anyway, as well as other small

isospin-breaking effects [66]). Since the amplitude zero appears at a center-of-mass momentum above the pion mass, it is unlikely that a pionless EFT can describe it. Our main goal here is to illustrate how RG invariance and PC work in a systematically improvable contact theory whose amplitude includes both a near-threshold pole and a low-energy zero. The great benefit of removing pions is simply to find analytical results, which cannot be reached if one includes OPE in (fully iterated) LO. Such results provide an important guide to the analysis of the pionful case we perform in Sec. III.

In the absence of explicit pions and nucleon excitations, all interactions among nucleons are of contact type. The part of the $\not\pi$EFT Lagrangian relevant for the NN $^1S_0$ channel is

$$\mathcal{L}_{\not\pi}^{(\mathrm{ct})} = N^\dagger\left(i\partial_0 + \frac{\boldsymbol{\nabla}^2}{2m_N}\right)N - C_0\left(N^T\vec{P}_{^1S_0}N\right)^\dagger\cdot\left(N^T\vec{P}_{^1S_0}N\right) + \cdots, \quad (1)$$

where N is the isodoublet, bispinor nucleon field and the NN $^1S_0$ projector is expressed in terms of the Pauli matrices $\boldsymbol{\sigma}$ ($\vec{\tau}$) acting on spin (isospin) space as $\vec{P}_{^1S_0} = \sigma_2\vec{\tau}\tau_2/\sqrt{8}$, while "$\cdots$" means more complicated interactions and relativistic corrections suppressed by negative powers of the breakdown scale of the theory. Now, the interaction term in Eq. (1) may be rewritten if, following Ref. [29], an auxiliary "dibaryon" field $\vec{\phi}$ with quantum numbers of an isovector pair of nucleons is introduced,

$$-C_0\left(N^T\vec{P}_{^1S_0}N\right)^\dagger\cdot\left(N^T\vec{P}_{^1S_0}N\right) \leftrightarrow \vec{\phi}^\dagger\cdot\Delta\vec{\phi} - g\left(\vec{\phi}^\dagger\cdot N^T\vec{P}_{^1S_0}N + \mathrm{H.c.}\right). \quad (2)$$

The dibaryon residual mass Δ and the dibaryon-NN coupling g are such that $C_0 = g^2/\Delta$, as can be straightforwardly checked if one performs the corresponding Gaussian path integral. This parameter redundancy permits the convenient choice [71]

$$g^2 \equiv \frac{4\pi}{m_N}. \quad (3)$$

Higher-order contact interactions can be reproduced by the inclusion of the dibaryon's kinetic term and derivative dibaryon-NN couplings.

The established PC of $\not\pi$EFT [16,17,60,61] accounts for the presence of a shallow virtual state at LO but does not produce as much energy dependence as the phenomenological phase shifts. A promotion of the dibaryon kinetic term to LO [64] allows for the reproduction of the derivative of the amplitude with respect to the energy around threshold. However, these approaches are equivalent to different truncations of the ERE and are unable to generate an amplitude zero. This is actually not a problem in $\not\pi$EFT, since k_0—numerically larger than m_π—is presumably outside the scope of this theory. But here we aim at reformulating the theory in a way such that k_0 is considered below the breakdown scale to illustrate the proposed reformulation of the χEFT PC in Sec. III.

Inspired by an EFT for nd scattering at very low energies [65], we consider here a generalization with *two* such dibaryon fields, $\vec{\phi}_{1,2}$,

FIG. 1. Full two-dibaryon propagator (solid box) resulting from the nonperturbative dressing of bare dibaryon-1 (dashed box) and dibaryon-2 (plain box) propagators with nucleon bubbles (circles).

$$\mathcal{L}_{\not\pi}^{(2\phi)} = N^\dagger\left(i\partial_0 + \frac{\boldsymbol{\nabla}^2}{2m_N}\right)N + \sum_{j=1,2}\vec{\phi}_j^\dagger\cdot\left[\Delta_j + c_j\left(i\partial_0 + \frac{\boldsymbol{\nabla}^2}{4m_N}\right)\right]\vec{\phi}_j - \sqrt{\frac{4\pi}{m_N}}\sum_{j=1,2}\left(\vec{\phi}_j^\dagger\cdot N^T\vec{P}_{^1S_0}N + \mathrm{H.c.}\right) + \cdots, \quad (4)$$

where we have made use of Eq. (3) and displayed explicitly the kinetic dibaryon terms with dimensionless factors c_j. As we will see, such an extension naturally allows us to reproduce the amplitude zero already at LO, greatly improving the description of the empirical phase shifts.

To illustrate the effects of the two dibaryons, we neglect for now the interactions represented by "$\cdots$" in Eq. (4). At momentum $k = \sqrt{m_N E}$, where E is the center-of-mass energy, the on-shell T matrix is written in terms of the S matrix and the phase shift δ as

$$T(k) = \frac{2\pi i}{m_N k}[S(k) - 1] = \frac{4\pi}{m_N}[-k\cot\delta(k) + ik]^{-1}. \quad (5)$$

Loops are regularized by a momentum cutoff Λ in the range $\Lambda \gtrsim M_{\mathrm{hi}} \gg k$ and a regulator function $f_R(q^2/\Lambda^2)$, with q the magnitude of the off-shell nucleon momentum, that satisfies

$$f_R(0) = 1, \quad f_R(\infty) = 0. \quad (6)$$

Computing the two-dibaryon self-energy, i.e., dressing up the bare two-dibaryon propagator

$$\mathcal{B}(k;\Lambda) = \sum_j\left[\Delta_j(\Lambda) + c_j(\Lambda)\frac{k^2}{m_N}\right]^{-1} \equiv \frac{m_N}{4\pi}V(k;\Lambda) \quad (7)$$

with nucleon loops (see Fig. 1), yields

$$\mathcal{D}(k;\Lambda) = \left[\frac{1}{\mathcal{B}(k;\Lambda)} + \mathcal{I}_0(k;\Lambda)\right]^{-1} \equiv \frac{m_N}{4\pi}T(k;\Lambda). \quad (8)$$

In this equation we introduced the regularized integral

$$\mathcal{I}_0(k;\Lambda) = 4\pi\int\frac{d^3q}{(2\pi)^3}\frac{f_R(q/\Lambda)}{q^2 - k^2 - i\epsilon} = ik + \theta_1\Lambda + \frac{k^2}{\Lambda}\sum_{n=0}^{\infty}\theta_{-1-2n}\left(\frac{k}{\Lambda}\right)^{2n}, \quad (9)$$

where the dimensionless coefficients θ_n depend on the specific regularization employed. For example, for a sharp-cutoff prescription with a step function it turns out that $\theta_n = 2/(n\pi)$, while in dimensional regularization with minimal subtraction

we have simply $\theta_n = 0$. We thus arrive at

$$\left[\frac{m_N}{4\pi}\,T(k;\Lambda)\right]^{-1} = \frac{[\Delta_1(\Lambda)+c_1(\Lambda)\,k^2/m_N][\Delta_2(\Lambda)+c_2(\Lambda)\,k^2/m_N]}{\Delta_1(\Lambda)+\Delta_2(\Lambda)+[c_1(\Lambda)+c_2(\Lambda)]\,k^2/m_N} + ik + \theta_1\Lambda + \theta_{-1}\frac{k^2}{\Lambda} + \mathcal{O}\left(\frac{k^4}{\Lambda^3}\right). \tag{10}$$

When k is much smaller than any other scale, this inverse amplitude reduces at large cutoff to the ERE,

$$\left[\frac{m_N}{4\pi}T(k)\right]^{-1} = \frac{1}{a} + ik - \frac{r_0}{2}k^2 - \frac{P_0}{4}k^4 + \cdots, \tag{11}$$

where, for neutron-proton (np) scattering, $a \simeq -23.7$ fm $\simeq -(8\text{ MeV})^{-1}$ [72] is the scattering length, $r_0 \simeq 2.7$ fm $\simeq (73\text{ MeV})^{-1}$ [73] is the effective range, $P_0 \simeq 2.0\text{ fm}^3 \simeq (158\text{ MeV})^{-3}$ [74] is the shape parameter, and so on. In addition, Eq. (10) allows for a pole at a momentum $k_0 \simeq 340$ MeV [63], around which the amplitude can be expanded as [61]

$$\frac{m_N}{4\pi}\,T(k) = \frac{k^2-k_0^2}{k_0^3}\left\{z_1 + z_2\frac{k^2-k_0^2}{k_0^2} + \mathcal{O}\left[\frac{(k-k_0)^2}{k_0^2}\right]\right\} \tag{12}$$

in terms of dimensionless parameters z_n, with $|z_n| = \mathcal{O}(1)$ in the absence of further fine-tuning. One can easily check that $\delta(k)$ behaves linearly around $k = k_0$, with a slope proportional to z_1,

$$\delta(k \sim k_0) = -\frac{2z_1}{k_0}(k-k_0) + \cdots. \tag{13}$$

From the Nijm93 phase shifts [63] we find $z_1 \simeq 0.6$.

It has long been recognized that the anomalously large value of $|a|$ is a consequence of a fine-tuning that places a virtual bound state very close to threshold and introduces an accidental, small-scale $\aleph \sim 10$ MeV corresponding to its binding momentum. In $\not\pi$EFT, higher ERE parameters are assumed to depend on a single higher-energy scale $\tilde{M}_{\rm hi}$, $1/r_0 \sim 1/P_0^{1/3} \sim \cdots = \mathcal{O}(\tilde{M}_{\rm hi})$. The PC then organizes the contributions to an observable characterized by a momentum $Q \sim \aleph$ in an expansion in powers of $Q/\tilde{M}_{\rm hi}$, i.e., $\tilde{M}_{\rm hi}$ is the breakdown scale of the theory. Naively one expects $\tilde{M}_{\rm hi} \lesssim m_\pi$, but there is some evidence that $\not\pi$EFT works also at larger momenta. For example, the binding momenta for the ground states of systems with $A = 3,4,6,16$ nucleons are near 100 MeV, and yet their physics is well described by the lowest orders of $\not\pi$EFT (see, for example, Refs. [75–78]). In fact, it has been suggested that the characteristic scale of $\not\pi$EFT is set by these binding momenta through the LO three-nucleon force, so that $\aleph$ appears only at NLO or higher [66,79].

Here we exploit a possible enlarged range of validity of $\not\pi$EFT in the $^1S_0$ channel to illustrate the idea of a low-energy zero. This can be done with the replacement $\tilde{M}_{\rm hi} \to M_{\rm lo}$. Simultaneously, we take into account the smallness of $1/a$ with the replacement $\aleph \to M_{\rm lo}^2/M_{\rm hi}$. The phenomenological parameters of the theory are assumed to scale as

$$1/a = \mathcal{O}\big(M_{\rm lo}^2/M_{\rm hi}\big), \quad k_0 \sim 1/r_0 \sim 1/P_0^{1/3} \sim \cdots = \mathcal{O}(M_{\rm lo}), \tag{14}$$

with $M_{\rm hi} \gg M_{\rm lo}$. This assumption will allow us to develop an expansion for an observable at typical momentum $Q \sim M_{\rm lo}$ in powers of $Q/M_{\rm hi}$. The usefulness of such an expansion is far from obvious, but as we show below it seems to give good results when compared to empirical low-energy data. Our prescription includes the correct position of the amplitude zero at LO and moves the virtual state at NLO very close to its empirical position. For $Q \sim \aleph$ the NLO amplitude is similar to that of standard $\not\pi$EFT with $\tilde{M}_{\rm hi} = \mathcal{O}(M_{\rm lo})$. The assignment $\aleph \to M_{\rm lo}^2/M_{\rm hi}$ is somewhat arbitrary but motivated by the expectation that $M_{\rm lo} \sim 100$ MeV and $M_{\rm hi} \sim 500$ MeV, when it holds within a factor of 2 or so. If $\aleph$ were taken to be smaller, then a reasonable description of observables at momenta $Q \sim \aleph$ would only emerge at higher orders. Conversely, had we decided to treat $\aleph$ as $M_{\rm lo}$, the very-low-energy region would be well reproduced already at LO, but it would be more difficult to see improvements at NLO.

Quantities in the theory can be organized in powers of the small expansion parameter $M_{\rm lo}/M_{\rm hi}$. For a generic coupling constant g, we expand formally

$$\mathsf{g}(\Lambda) = \mathsf{g}^{[0]}(\Lambda) + \mathsf{g}^{[1]}(\Lambda) + \cdots, \tag{15}$$

where the superscript $^{[\nu]}$ indicates that the coupling appears at N$^\nu$LO. The "renormalized" coupling $\bar{\mathsf{g}}^{[\nu]}$—i.e., the regulator-independent contribution to the bare (running) coupling $\mathsf{g}^{[\nu]}(\Lambda)$—is nominally suppressed by $\mathcal{O}(M_{\rm lo}^\nu/M_{\rm hi}^\nu)$ with respect to $\bar{\mathsf{g}}^{[0]}$.

Likewise, the amplitude is written

$$T(k;\Lambda) = T^{[0]}(k;\Lambda) + T^{[1]}(k;\Lambda) + \cdots, \tag{16}$$

where

$$T^{[0]}(k;\Lambda) = V^{[0]}(k;\Lambda)\left[1 + \frac{m_N}{4\pi}V^{[0]}(k;\Lambda) \times\left(ik + \theta_1\Lambda + \frac{k^2}{\Lambda}\sum_{n=0}^{\infty}\theta_{-1-2n}\frac{k^{2n}}{\Lambda^{2n}}\right)\right]^{-1}, \tag{17}$$

$$T^{[1]}(k;\Lambda) = \left[\frac{T^{[0]}(k;\Lambda)}{V^{[0]}(k;\Lambda)}\right]^2 V^{[1]}(k;\Lambda), \tag{18}$$

etc., in terms of

$$V^{[0]}(k;\Lambda) = \frac{4\pi}{m_N}\sum_j\left[\Delta_j^{[0]}(\Lambda) + c_j^{[0]}(\Lambda)\frac{k^2}{m_N}\right]^{-1}, \tag{19}$$

$$V^{[1]}(k;\Lambda) = -\frac{4\pi}{m_N}\sum_j\left[\Delta_j^{[0]}(\Lambda) + c_j^{[0]}(\Lambda)\frac{k^2}{m_N}\right]^{-2} \times\left[\Delta_j^{[1]}(\Lambda) + c_j^{[1]}(\Lambda)\frac{k^2}{m_N}\right], \tag{20}$$

etc. Neglecting higher-order terms, the phase shifts at LO, LO+NLO, and so on can be written as

$$\delta^{[0]}(k;\Lambda) = -\cot^{-1}\left\{\frac{4\pi}{m_N k}\,\mathrm{Re}[\,T^{[0]}(k;\Lambda)]^{-1}\right\}, \quad (21)$$

$$\delta^{[0+1]}(k;\Lambda) = -\cot^{-1}\left(\frac{4\pi}{m_N k}\,\mathrm{Re}\left\{[T^{[0]}(k;\Lambda)]^{-1} \times\left[1-\frac{T^{[1]}(k;\Lambda)}{T^{[0]}(k;\Lambda)}\right]\right\}\right), \quad (22)$$

etc. At higher orders interactions in the "$\cdots$" of Eq. (4) appear. We now consider the first two orders of the expansion in detail.

A. Leading order

From Eq. (10) we see that reproducing the amplitude zero at LO with a shallow pole requires a minimum of three bare parameters. Both residual masses, $\Delta_1(\Lambda)$ and $\Delta_2(\Lambda)$, must be nonvanishing; otherwise, the resulting inverse amplitude at threshold would be proportional to Λ, i.e., not properly renormalized. At the same time, at least one of the kinetic factors, which we choose to be $c_2(\Lambda)$, needs to appear at LO; otherwise, the amplitude zero could not be reproduced.

Since we attribute in Eq. (14) the smallness of the inverse scattering length to a suppression by one power of the breakdown scale $M_{\rm hi}$, we take

$$\frac{1}{a^{[0]}} = 0. \quad (23)$$

In other words, we perform an expansion of the NN $^1S_0$ amplitude around the unitarity limit, as in Refs. [66,79]. One of the dibaryon parameters, which turns out to be $\Delta_2(\Lambda)$, carries such an effect, so that its observable contribution vanishes at LO. The regulator-independent parts of the remaining LO parameters, Δ_1 and c_2, are assumed to be governed by the scale $M_{\rm lo}$.[2] In a nutshell,

$$\bar{\Delta}_1^{[0]} = \mathcal{O}(M_{\rm lo}), \quad \frac{\bar{c}_1^{[0]}}{m_N} = 0, \quad \bar{\Delta}_2^{[0]} = 0, \quad \frac{\bar{c}_2^{[0]}}{m_N} = \mathcal{O}\left(\frac{1}{M_{\rm lo}}\right). \quad (24)$$

Because of the vanishing of $c_1^{[0]}$, eliminating dibaryon-1 via Eq. (2) generates a momentum-independent contact interaction. Thus, at LO we obtain—except for our additional requirement (23)—the $M_{NN}\to\infty$ version of the model considered in Ref. [29], where a dibaryon (our dibaryon-2) is added to a series of nucleon contact interactions.

In order to relate $\Delta_1^{[0]}(\Lambda)$, $\Delta_2^{[0]}(\Lambda)$, and $c_2^{[0]}(\Lambda)$—our three nonvanishing LO bare parameters—to observables, we impose on

$$F(z;\Lambda) \equiv \mathrm{Re}\left\{\left[\frac{m_N}{4\pi}\,T^{[0]}(\sqrt{z};\Lambda)\right]^{-1}\right\} \quad (25)$$

three renormalization conditions,

$$F(0;\Lambda) = 0, \quad \left.\frac{\partial F(z;\Lambda)}{\partial z}\right|_{z=0} = -\frac{r_0}{2}, \quad F^{-1}(k_0^2;\Lambda) = 0. \quad (26)$$

The dependence of loops on positive powers of Λ is canceled by that of the bare couplings, which is given in Appendix. Equation (24) ensures that the nonvanishing renormalized couplings,

$$\bar{\Delta}_1^{[0]} = \frac{r_0 k_0^2}{2}, \quad \frac{\bar{c}_2^{[0]}}{m_N} = -\frac{r_0}{2}, \quad (27)$$

are indeed consistent with Eq. (14). Apart from a residual cutoff dependence that can be made arbitrarily small by increasing the cutoff, the amplitude can now be expressed in terms of the renormalized couplings or, using Eq. (27), in terms of r_0 and k_0:

$$\left[\frac{m_N}{4\pi}\,T^{[0]}(k;\Lambda)\right]^{-1} = ik - \frac{r_0}{2}\frac{k^2}{1-k^2/k_0^2}\left(1+\frac{2\theta_{-1}}{r_0\Lambda}\,\frac{k^2}{k_0^2}\right) + \mathcal{O}\left(\frac{k^4}{\Lambda^3}\right). \quad (28)$$

Although the scales and the zero location are different, Eq. (28) is similar to the one [65] for nd scattering at very low energies.[3]

Many interesting consequences can be extracted from Eq. (28). For momenta below the amplitude zero, our expression reduces to the unitarity-limit version of the ERE (11) but with predictions for the higher ERE parameters, starting with the shape parameter

$$P_0^{[0]}(\Lambda) = \frac{2r_0}{k_0^2}\left[1+\frac{2\theta_{-1}}{r_0\Lambda}+\mathcal{O}\left(\frac{k_0^2}{r_0\Lambda^3}\right)\right]. \quad (29)$$

Using the cutoff dependence to estimate the error under the assumption $M_{\rm hi}\sim 500$ MeV, the LO prediction is $P_0^{[0]}k_0^2/(2r_0) = 1.0\pm 0.3$. These high ERE parameters are difficult to extract from data. A careful analysis in Ref. [74] obtains $P_0 k_0^2/(2r_0) = 1.1$, which is well within our expected truncation error. Yet values obtained for P_0 from the phenomenological np potentials NijmII and Reid93 [70] are of the same order of magnitude as the value from Ref. [74], but with a *negative* sign [81].

We conjecture that, in contrast to what happens in standard $\not\pi$EFT, Eq. (28) also applies at momenta around the amplitude zero, with terms which are $\mathcal{O}(M_{\rm lo})$ and corrections of $\mathcal{O}(M_{\rm lo}^2/M_{\rm hi})$. Around the amplitude zero, the amplitude is perturbative [37,61]. Indeed, a simple Taylor expansion of Eq. (28) gives a perturbative expansion in the region

[2] NDA [7,8] gives for a dibaryon-NN coupling $g=\mathcal{O}(4\pi/\sqrt{m_N})$, which differs from our convention (3) by a factor of $\sqrt{4\pi}$. Since it is the combination g^2/Δ that enters the amplitude, Δ is expected to be $\mathcal{O}(M_{\rm hi}/(4\pi)) = \mathcal{O}(M_{\rm lo})$ instead of $\mathcal{O}(M_{\rm hi})$.

[3] Defining

$$A \equiv \frac{r_0}{2}k_0^2 \equiv -R,$$

Eq. (28) may be rewritten as

$$\left[\frac{m_N}{4\pi}\,T^{[0]}(k;\Lambda)\right]^{-1} = A + \frac{R}{1-k^2/k_0^2} + ik + \mathcal{O}\left(\frac{k^2}{\Lambda}\right),$$

which is a form used in early work on nd scattering, such as Ref. [80].

$|k-k_0| \lesssim k_0$, i.e., an equation of the form (12) with LO predictions for the coefficients,

$$z_1^{[0]}(\Lambda) = \frac{2}{r_0 k_0}\left(1 - \frac{2\theta_{-1}}{r_0\Lambda} + \cdots\right), \tag{30}$$

$$z_2^{[0]}(\Lambda) = -\frac{2}{r_0 k_0}\left[1 + \frac{2i}{r_0 k_0}\left(1 - \frac{4\theta_{-1}}{r_0\Lambda}\right) + \cdots\right], \tag{31}$$

where the "$\cdots$" account for $\mathcal{O}(M_{\rm lo}^2/\Lambda^2)$. Numerically, these coefficients are $z_1^{[0]} = 0.4 \pm 0.1$ and $z_2^{[0]} = -(0.4 \pm 0.1) - i(0.2 \pm 0.1)$, which are indeed of $\mathcal{O}(1)$. The former is in fact reasonably close to $z_1 \simeq 0.6$ extracted from the phenomenological data. Note that we could have imposed as a renormalization condition that z_1 had a fixed value—the one that best fits the empirical value—at any Λ, thus trading the information about energy dependence carried by r_0 for that contained in the derivative of the phase shift at its zero, see Eq. (13).

Equation (28) interpolates between the two regions, $k \ll k_0$ where the amplitude is nonperturbative and $|k-k_0| \ll k_0$ where it is perturbative. Compared to standard $\not\pi$EFT, it resums not only range corrections as in Ref. [64] but also corrections that give rise to the pole at $k = k_0$. Compared to the expansion around the amplitude zero [61], it resums the terms that become large at low energies and give rise to a resonant state at zero energy. The pole structure of the LO amplitude can be made explicit by rewriting Eq. (28) as

$$\left[\frac{m_N}{4\pi}\,T^{[0]}(k;\Lambda)\right]^{-1} = \frac{\left(k - i\kappa_1^{[0]}\right)\left(k - i\kappa_2^{[0]}\right)\left(k - i\kappa_3^{[0]}\right)}{i\left(k_0^2 - k^2\right)} + \mathcal{O}\left(\frac{k^2}{\Lambda}\right), \tag{32}$$

with

$$\kappa_1^{[0]} = 0, \quad \kappa_2^{[0]} = \frac{r_0 k_0^2}{4}\left\{1 - \sqrt{1 - [4/(r_0 k_0)]^2}\right\},$$
$$\kappa_3^{[0]} = \frac{r_0 k_0^2}{4}\left\{1 + \sqrt{1 - [4/(r_0 k_0)]^2}\right\}. \tag{33}$$

In addition to the amplitude zero, $T^{[0]}(k_0;\Lambda) = 0$, it is apparent that there are three simple poles, $T^{[0]}(i\kappa_j^{[0]};\infty) \to \infty$, the nature of which is linked to the sign of $i\,\mathrm{Res}\,S^{[0]}(i\kappa_j^{[0]})$:

(i) The pole at $k = 0$ represents a resonant state at threshold, as it induces the vanishing of $\cot\delta(0)$. Such a pole can be reproduced even with a momentum-independent contact potential, just as it is done at LO in standard $\not\pi$EFT (1) in the unitarity limit. (Since $i\,\mathrm{Res}\,S^{[0]}(i\kappa_1^{[0]}) = 0$, this state has a non-normalizable wave function.)

(ii) The pole at $k = i\kappa_2^{[0]}$, $\kappa_2^{[0]} \simeq 190$ MeV, lies on the positive imaginary semiaxis. However, since $i\,\mathrm{Res}\,S^{[0]}(i\kappa_2^{[0]}) < 0$, the condition to produce a normalizable wave function is not satisfied. The pole at $k = i\kappa_2^{[0]}$ cannot correspond to a bound state whose wave function has finite support in coordinate space. It is a *redundant* pole [82,83].

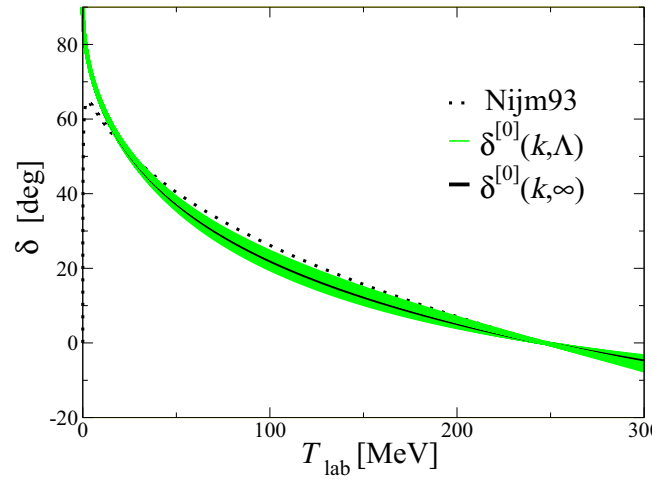

FIG. 2. np $^1S_0$ phase shift δ (in degrees) versus laboratory energy $T_{\rm lab} = 2k^2/m_N$ (in MeV) for $\not\pi$EFT at LO in our new PC. The (black) solid line shows the analytical result (28) with $\Lambda \to \infty$, while the (green) band around it represents the evolution of the cutoff from 500 MeV to infinity, with $\theta_{-1} = \pm 1$. The (black) squares are the Nijm93 results [63,70].

(iii) The pole at $k = i\kappa_3^{[0]}$, $\kappa_3^{[0]} \simeq 600$ MeV, lies deep on the positive imaginary semiaxis. It represents a bound state because $i\,\mathrm{Res}\,S^{[0]}(i\kappa_3^{[0]}) > 0$. Since no such state exists experimentally, it would set an upper bound on the regime of validity of this hypothetical EFT, $M_{\rm hi} \lesssim \kappa_3^{[0]}$.

In Fig. 2, we plot the $^1S_0$ phase shifts (21) from the LO amplitude (28) in comparison with the Nijm93 results [63,70]. As input, we use the empirical values of the effective range and the position of the amplitude zero. We display the cutoff band for a generic regulator by taking $\theta_{-1} = \pm 1$ and varying Λ from around the breakdown scale (500 MeV) to infinity—as the cutoff increases, our results converge, as evident in Eq. (28). This cutoff band provides an estimate of the LO error, except at low momentum where there is an error that scales with $1/|a|$ instead of k. The LO phase shifts are in good agreement with empirical values for most of the low-energy momentum range, except at the very low momenta where the small but nonvanishing virtual-state binding energy is noticeable. A plot of $k\cot\delta$ shows that differences at the amplitude level are indeed small. We plot phase shifts to better display the region around the amplitude zero, which our PC is designed to capture. There, while the phase shifts themselves are not too far off empirical values, the curvature is not well reproduced. Nevertheless, the agreement is surprisingly good given the absence of explicit pion fields. In the next section we examine how robust this agreement is.

B. Next-to-leading order

As pointed out in Ref. [26], the leading residual cutoff dependence of an amplitude, together with the assumption of naturalness, gives an upper bound on the order of the next correction to that amplitude. In standard $\not\pi$EFT, for example,

the LO amplitude has an effective range $r_0 \sim 1/\Lambda$, indicating that there is an interaction at order no higher than NLO [16,17,60,61] which will produce a physical effective range $r_0 \sim 1/\tilde{M}_{\rm hi}$. The leading residual cutoff dependence in Eq. (28) is proportional to k^4 and of relative order $\mathcal{O}(M_{\rm lo}/\Lambda)$. Thus, the NLO interaction must give rise to a contribution

$$P_0^{[1]}(\Lambda) \equiv P_0 - P_0^{[0]}(\Lambda) = \mathcal{O}\left(\frac{1}{M_{\rm lo}^2 M_{\rm hi}}\right) \tag{34}$$

to the LO shape parameter (29). This correction requires a higher-derivative operator. Although we could add a momentum-dependent contact operator, a simpler, energy-dependent strategy will be implemented here: We allow for a nonvanishing $c_1^{[1]}$.

In addition, since we are interpreting $\aleph \to M_{\rm lo}^2/M_{\rm hi}$, one combination of parameters including $\Delta_2^{[1]}$ enforces

$$\frac{1}{a^{[1]}} = \frac{1}{a} = \mathcal{O}\left(\frac{M_{\rm lo}^2}{M_{\rm hi}}\right). \tag{35}$$

We also introduce corrections in the other two parameters, $c_2^{[1]}$ and $\Delta_1^{[1]}$, in order to keep r_0 and k_0 unchanged. Since NLO interactions must all be suppressed by $M_{\rm hi}^{-1}$,

$$\bar{\Delta}_1^{[1]} = \mathcal{O}\left(\frac{M_{\rm lo}^2}{M_{\rm hi}}\right), \quad \frac{\bar{c}_1^{[1]}}{m_N} = \mathcal{O}\left(\frac{1}{M_{\rm hi}}\right), \quad \bar{\Delta}_2^{[1]} = \mathcal{O}\left(\frac{M_{\rm lo}^2}{M_{\rm hi}}\right),$$
$$\frac{\bar{c}_2^{[1]}}{m_N} = \mathcal{O}\left(\frac{1}{M_{\rm hi}}\right). \tag{36}$$

This scaling—together with what was learned at LO—is consistent with the imposition of four renormalization conditions on

$$G(z;\Lambda) \equiv -{\rm Re}\left\{\left[\frac{m_N}{4\pi}T^{[1]}(\sqrt{z};\Lambda)\right]\left[\frac{m_N}{4\pi}T^{[0]}(\sqrt{z};\Lambda)\right]^{-2}\right\}, \tag{37}$$

which ensure that a, r_0, P_0, and k_0 are fully Λ independent at NLO:

$$G(0;\Lambda) = \frac{1}{a}, \quad \left.\frac{\partial G(z;\Lambda)}{\partial z}\right|_{z=0} = 0,$$
$$\left.\frac{\partial^2 G(z;\Lambda)}{\partial z^2}\right|_{z=0} = -\frac{P_0^{[1]}(\Lambda)}{2}, \quad G(k_0^2;\Lambda) = 0. \tag{38}$$

The cutoff dependence of the bare parameters that guarantees Eq. (38) can be found in Appendix. With Eq. (36), the renormalized parameters

$$\bar{\Delta}_1^{[1]} = \bar{\Delta}_2^{[1]} + \frac{3k_0^2}{m_N}\bar{c}_1^{[1]}, \quad \frac{\bar{c}_1^{[1]}}{m_N} = -\frac{r_0}{2}\left(1 - \frac{P_0 k_0^2}{2r_0}\right),$$
$$\bar{\Delta}_2^{[1]} = \frac{1}{a} + r_0 k_0^2\left(1 - \frac{P_0 k_0^2}{2r_0}\right), \quad \frac{\bar{c}_2^{[1]}}{m_N} = -4\left(\frac{\bar{c}_1^{[1]}}{m_N} + \frac{\bar{\Delta}_2^{[1]}}{2k_0^2}\right), \tag{39}$$

give Eqs. (14) and (34). The NLO contribution to the amplitude, Eq. (18), then satisfies

$$\frac{T^{[1]}(k;\Lambda)}{T^{[0]2}(k;\Lambda)} = -\frac{m_N}{4\pi}\left[\frac{1}{a} + \frac{r_0}{2k_0^2}\frac{k^4}{1-k^2/k_0^2} \times\left(1 - \frac{P_0 k_0^2}{2r_0} + \frac{2\theta_{-1}}{r_0\Lambda}\right) + \mathcal{O}\left(\frac{k^4}{\Lambda^3}\right)\right], \tag{40}$$

which is indeed suppressed by one negative power of $M_{\rm hi}$. If we resum $T^{[1]}(k;\Lambda)$ while neglecting N^{2}LO corrections, then

$$\left\{\frac{m_N}{4\pi}[T^{[0]}(k;\Lambda) + T^{[1]}(k;\Lambda)]\right\}^{-1} = \frac{1}{a} + ik - \frac{r_0}{2}k^2 - \frac{P_0}{4}\frac{k^4}{1-k^2/k_0^2} + \mathcal{O}\left(\frac{k^6}{k_0^2\Lambda^3}\right). \tag{41}$$

Now the ERE (11) is reproduced for $k < k_0$ with the experimental scattering length and shape parameter. Additionally, there are predictions for the higher ERE parameters which are hard to test directly since they are difficult to extract from data. The zero at k_0 remains unchanged due to our choice of renormalization condition. Once expanded around $k = k_0$, the distorted amplitude (41) yields NLO coefficients such as

$$z_1^{[1]}(\Lambda) = z_1^{[0]}(\infty)\left(1 - \frac{P_0 k_0^2}{2r_0}\right) + \cdots, \tag{42}$$

$$z_2^{[1]}(\Lambda) = z_2^{[0]}(\infty)\left(1 - i\,\frac{r_0 k_0}{2}\right)^{-1} \times\left[2\left(1 - \frac{P_0 k_0^2}{2r_0}\right) - \frac{i}{ak_0}\right] + \cdots, \tag{43}$$

where "$\cdots$" stands for $\mathcal{O}(M_{\rm lo}^3/\Lambda^3)$. NLO contributions are of relative $\mathcal{O}(M_{\rm lo}/M_{\rm hi})$ with respect to their LO predictions $z_1^{[0]}$ and $z_2^{[0]}$, consistently with the residual cutoff dependence displayed in Eqs. (30) and (31). Since $z_1^{[0]}(\infty)$ underestimates the slope of the phenomenological phase shifts around the amplitude zero, a better description of data requires $z_1^{[1]}(\infty) > 0$ and, thus, according to Eqs. (29) and (42), $P_0 \lesssim P_0^{[0]}(\infty)$. The value given in Ref. [74] leads to a small change $|z_{1,2}^{[1]}(\infty)/z_{1,2}^{[0]}(\infty)| \lesssim 1/10$, but unfortunately it is $\sim$10% *larger* than $P_0^{[0]}(\infty)$. Since Ref. [74] provides no error bars it is difficult to decide whether this is a real problem. We can reproduce the phenomenological value for z_1 with $P_0^{[1]}(\infty) \simeq -0.6\,P_0^{[0]}(\infty)$, which is still compatible with convergence but not so small a change with respect to LO. Of course, not all the discrepancy between LO and phenomenology should come from NLO, but this might be indicative that something is missing. We will return to the shape parameter in the next section.

NLO also shifts the LO position of the poles (33) of the S matrix. One can obtain these shifts reliably by means of perturbative tools only for the two shallowest LO poles, finding in the large-cutoff limit

$$\kappa_1^{[1]} = \frac{1}{a},$$
$$\kappa_2^{[1]} = -\frac{k_0^2 + \kappa_2^{[0]2}}{k_0^2 - \kappa_2^{[0]2}}\left[\frac{1}{a} + \frac{1}{2}\frac{r_0\kappa_2^{[0]4}}{k_0^2 + \kappa_2^{[0]2}}\left(1 - \frac{P_0 k_0^2}{2r_0}\right)\right]. \tag{44}$$

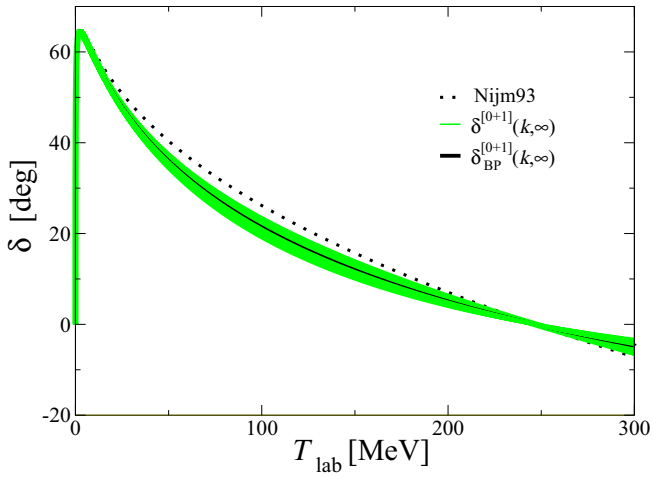

FIG. 3. np $^1S_0$ phase shift δ (in degrees) versus laboratory energy $T_{\rm lab} = 2k^2/m_N$ (in MeV) for $\not\pi$EFT at NLO in our new PC. The (black) line shows the analytical result (40) with $\Lambda \to \infty$ and the value of the shape parameter from Ref. [74], while the (green) band around it represents a $\pm 30\%$ variation in this value. The (black) squares are the Nijm93 results [63,70].

We see that, as expected, $|\kappa_1^{[1]}| \sim |\kappa_2^{[1]}| = \mathcal{O}(M_{\rm lo}^2/M_{\rm hi})$, as long as $\kappa_2^{[0]} = \mathcal{O}(M_{\rm lo})$. As a consequence:

(i) The shallowest pole is moved from threshold to $k \simeq -8i$ MeV and represents the well-known virtual state. Its new location almost coincides with the physical one.
(ii) The redundant pole is moved from $k \simeq 190i$ MeV to $k \simeq 215i$ MeV, when the value of P_0 given in Ref. [74] is used. This represents a shift of relative size $\sim$15% with respect to LO. Roughly two thirds of this shift are due to the finiteness of the scattering length, while the other third corresponds to the NLO correction to the shape parameter. If we take the value of P_0 that gives the slope of the phenomenological phase shifts at k_0, then the shape correction overcomes the scattering length and the pole moves to $k \simeq 155i$ MeV, still a modest shift.

The LO+NLO $^1S_0$ phase shift can now be obtained from Eqs. (22) and (40), see Fig. 3. Now, in addition to the empirical values of r_0 and k_0, also the values of the scattering length and the shape parameter from Ref. [74] are input. We show a band corresponding to a variation of $\pm 30\%$ around the P_0 value of Ref. [74] to account for its (unspecified) error. Since the cutoff dependence of the NLO result (40) is very quickly convergent ($\sim 1/\Lambda^3$), it has been neglected in Fig. 3. The band thus does not reflect the uncertainty of the NLO truncation, but of the input.

As expected, the physical value of a greatly improves the description of the phase shifts at low energies ($k \lesssim 50$ MeV). However, at middle energies ($k \sim 100$ MeV) this improvement is much less clear. In particular, as anticipated above, only for a shape parameter $\sim$30% smaller than in Ref. [74] does $\delta^{[0+1]}(k;\infty)$ get slightly closer to empirical values than $\delta^{[0]}(k;\infty)$ (see Fig. 2). Such a change is within the LO error and, overall, the reproduction of the phase shifts is very good at NLO. Agreement could be further improved, particularly around k_0, by taking an even smaller value for the shape parameter—in particular, the value that reproduces the phenomenological value for z_1. However, even in that case the curvature of the resulting phase shifts would remain different from empirical at middle energies, which suggests that our expansion is lacking terms at either LO or NLO.

C. Resummation and higher orders

The choice of identifying the fine-tuning scale $\aleph$ with $M_{\rm lo}^2/M_{\rm hi}$ led to a finite scattering length only at NLO. This assignment is motivated by the numerical values estimated for these scales. Alternative choices are possible, leading to slightly different amplitudes at various orders. When plotting phase shifts, these differences are amplified. For example, taking $\aleph$ as $M_{\rm lo}$ leads to a renormalization condition where $1/a$ is nonzero already at LO. In this case our running and renormalized parameters given above all change by $1/a$ terms. The amplitude itself (or, equivalently, its pole positions) changes only slightly, but in terms of phase shifts there appears to be a large improvement.

Given our previous identification of $\aleph$ with $M_{\rm lo}^2/M_{\rm hi}$, the alternative procedure just described amounts to a resummation of higher-order corrections. Because a bare parameter $[\Delta_2(\Lambda)]$ exists already at LO to ensure proper renormalization, this resummation can be done without harm. However, because some NLO contributions are shifted to LO, we see less improvement when going from LO to NLO. Provided that one has a PC that converges, this is just one of many ways in which we can make results at one order closer to phenomenology while remaining within the error of that order.

Regardless of such resummation, corrections at higher orders are expected to improve the situation further. The cutoff dependence of Eq. (41) suggests that there are no new interactions at next order, N^{2}LO, which would solely consist of one iteration of the NLO potential. However, the fact that our pionless phase shifts look too low in the middle range represents a significant, systematic lack of attraction between nucleons at $k \sim m_\pi$. This could be a reminder to include pions explicitly. We now consider our expansion with additional pion exchange.

III. PIONFUL THEORY

We now modify the theory developed in the previous section to include pion exchange. This is done under the assumption that the pion mass, the characteristic inverse strength of OPE, and the magnitude of the relevant momenta have similar sizes, not being enhanced or suppressed by powers of the hard scale:

$$m_\pi \sim M_{NN} \sim Q = \mathcal{O}(M_{\rm lo}). \tag{45}$$

Such an assumption has been standard in χEFT since its beginnings [4,5]. In the NN sector, it underlies the (nonperturbative) LO character of the OPE interaction, as well as the suppression of multiple pion exchanges by powers of $(M_{\rm lo}/M_{\rm QCD})^2$. Here, the fact that numerically $M_{NN} \simeq 290$ MeV suggests that the zero of the $^1S_0$ amplitude at $k_0 \simeq 340$ MeV might be

considered a low-energy scale as well. Note that certain spin-triplet channels—particularly $^3S_1$ and $^3P_0$—also display amplitude zeros at comparable momenta. In these channels the presence of the tensor force is sufficient to ensure a qualitatively correct description of the phase shifts already at LO in a power counting consistent with RG invariance [10,24,25]. This is in contrast with $^1S_0$ [26], where the amplitude zero appears only for low momentum cutoff values on the order of $M_{\rm lo}$ [22].

The Coulomb interaction between protons—the dominant electromagnetic effect—contributes an expansion in $\alpha m_N/M_{\rm lo} \sim \aleph/M_{\rm lo}$, where $\alpha \simeq 1/137$ is the fine-structure constant. As we took $\aleph = \mathcal{O}(M_{\rm lo}^2/M_{\rm hi})$, we should account for the Coulomb interaction at NLO. (Other isospin-breaking effects, such as the nucleon mass splitting, are to be accounted for perturbatively, too.) Within the $\not\pi$EFT framework, the (subleading) Coulomb effects were included in an expansion around the unitarity limit (without consideration of the amplitude zero) in Ref. [66]. Since we anticipate no new features here, in this first approach we neglect isospin breaking. We also ignore the explicit dependence on quark mass, because the expansion is already quite complicated at a fixed value of m_π^2.

Pions are introduced in the usual way by demanding that the most general effective Lagrangian transforms under chiral symmetry as does the QCD Lagrangian written in terms of quarks and gluons. (For reviews and references, see Refs. [1–3].) In the particular case of one dibaryon field, this was done in Ref. [29]. The extension to the two dibaryons of the previous section is straightforward. If $\vec\pi$ is the pion isotriplet, then the effective Lagrangian reads

$$\begin{aligned}\mathcal{L}_\chi^{(2\phi)} &= \frac{1}{2}\left(\partial_\mu\vec\pi\cdot\partial^\mu\vec\pi - m_\pi^2\vec\pi^{\,2}\right)\\ &+ N^\dagger\left[i\partial_0 + \frac{\boldsymbol\nabla^2}{2m_N} - \frac{g_A}{2f_\pi}\vec\tau\cdot(\boldsymbol\sigma\cdot\boldsymbol\nabla\vec\pi)\right]N\\ &+ \sum_{j=1,2}\left\{\vec\phi_j^{\,\dagger}\cdot\left[\Delta_j + c_j\left(i\partial_0 + \frac{\boldsymbol\nabla^2}{4m_N}\right)\right]\vec\phi_j\right.\\ &\left. - \sqrt{\frac{4\pi}{m_N}}\left(\vec\phi_j^{\,\dagger}\cdot N^T\vec P_{^1S_0}N + \text{H.c.}\right)\right\} + \cdots, \end{aligned} \tag{46}$$

in the same notation as Eq. (4). The omitted terms, which include chiral partners of the terms shown explicitly, are not needed up to NLO.

Inspired by the pionless theory, we use for the pionful case the same dibaryon arrangement of short-range potentials as in Sec. II. Adding the long-range, spin-singlet projection of OPE, the LO potential is

$$\begin{aligned}\frac{m_N}{4\pi}V^{[0]}(\boldsymbol p',\boldsymbol p,k;\Lambda) &= -\frac{m_\pi^2}{M_{NN}}\frac{1}{(\boldsymbol p'-\boldsymbol p)^2+m_\pi^2} + \frac{1}{\Delta_1^{[0]}(\Lambda)}\\ &\quad + \frac{1}{\Delta_2^{[0]}(\Lambda)+c_2^{[0]}(\Lambda)\,k^2/m_N}\\ &\equiv \frac{m_N}{4\pi}\left[V_{\rm L}^{[0]}(\boldsymbol p',\boldsymbol p) + V_{\rm S}^{[0]}(k;\Lambda)\right], \end{aligned} \tag{47}$$

where $\boldsymbol p$ ($\boldsymbol p'$) is the relative incoming (outgoing) momentum and the inverse OPE strength is defined as [16,17]

$$M_{NN} \equiv \frac{16\pi f_\pi^2}{g_A^2 m_N} \approx 290\ \text{MeV}. \tag{48}$$

The momentum-independent, contact piece of OPE has been absorbed in the short-range potential $V_{\rm S}^{[0]}$ through the redefinition

$$\left[1/\Delta_1^{[0]}(\Lambda) + 1/M_{NN}\right]^{-1} \to \Delta_1^{[0]}(\Lambda). \tag{49}$$

The long-range part of OPE is the Yukawa potential represented by $V_{\rm L}^{[0]}$. Integrating out dibaryon-1 we obtain the potential considered previously in Ref. [29]. Since two-pion exchange (TPE) enters only at N^{2}LO and higher [18,19], at NLO the interaction is entirely short-ranged,

$$\begin{aligned}\frac{m_N}{4\pi}V^{[1]}(k;\Lambda) &= -\frac{\Delta_1^{[1]}(\Lambda)+c_1^{[1]}(\Lambda)\,k^2/m_N}{\Delta_1^{[0]2}(\Lambda)}\\ &\quad - \frac{\Delta_2^{[1]}(\Lambda)+c_2^{[1]}(\Lambda)\,k^2/m_N}{\left[\Delta_2^{[0]}(\Lambda)+c_2^{[0]}(\Lambda)\,k^2/m_N\right]^2}. \end{aligned} \tag{50}$$

In the limit $\Delta_2^{[0]} \to \infty$ the potential is an energy-dependent version of the momentum-dependent LO+NLO interaction of Ref. [26], while the interaction of Ref. [54] emerges in the limit $\Delta_1^{[0]} \to \infty$.

Because OPE cannot be iterated analytically to all orders, we can no longer show explicitly that the amplitude has a zero at LO or that the amplitude is RG invariant. However, these two important features of the pionless theory are expected to be retained by the pionful theory on the basis that the strength of OPE is known to be numerically moderate in spin-singlet channels and that $V_{\rm L}^{[0]}$ is nonsingular. Moreover, we continue to use the scalings (24) and (36). Below we confirm through numerical calculations that the EFT obeying such a PC indeed has an amplitude zero and preserves RG invariance.

A. Leading order

The off-shell LO amplitude is found from the LO potential (47) by solving the LS equation

$$T^{[0]}(\boldsymbol p',\boldsymbol p,k;\Lambda) = V^{[0]}(\boldsymbol p',\boldsymbol p,k;\Lambda) - m_N\int\frac{d^3q}{(2\pi)^3}\frac{f_R(q/\Lambda)}{q^2-k^2-i\epsilon}V^{[0]}(\boldsymbol p',\boldsymbol q,k;\Lambda)\,T^{[0]}(\boldsymbol q,\boldsymbol p,k;\Lambda), \tag{51}$$

with $f_R(q/\Lambda)$ a nonlocal regulator function (6). Defining the Yukawa amplitude,

$$T_{\rm L}^{[0]}(\boldsymbol p',\boldsymbol p,k;\Lambda) = V_{\rm L}^{[0]}(\boldsymbol p',\boldsymbol p) - m_N\int\frac{d^3q}{(2\pi)^3}\frac{f_R(q/\Lambda)}{q^2-k^2-i\epsilon}V_{\rm L}^{[0]}(\boldsymbol p',\boldsymbol q)\,T_{\rm L}^{[0]}(\boldsymbol q,\boldsymbol p,k;\Lambda), \tag{52}$$

the Yukawa dressing of the incoming/outgoing NN states,

$$\chi_{\rm L}^{[0]}(\boldsymbol{p},k;\Lambda) = 1 - m_N \int \frac{d^3q}{(2\pi)^3} \frac{f_R(q/\Lambda)}{q^2-k^2-i\epsilon}\, T_{\rm L}^{[0]}(\boldsymbol{p},\boldsymbol{q},k;\Lambda), \tag{53}$$

and the resummation of NN bubbles with iterated OPE in the middle,

$$\mathcal{I}_{\rm L}^{[0]}(k;\Lambda) = 4\pi \int \frac{d^3q}{(2\pi)^3} \frac{f_R(q/\Lambda)}{q^2-k^2-i\epsilon}\, \chi_{\rm L}^{[0]}(\boldsymbol{q},k;\Lambda), \tag{54}$$

Eq. (51) can be rewritten as [9]

$$\left\{\frac{m_N}{4\pi}\left[T^{[0]}(\boldsymbol{p}',\boldsymbol{p},k;\Lambda) - T_{\rm L}^{[0]}(\boldsymbol{p}',\boldsymbol{p},k;\Lambda)\right]\right\}^{-1} = \frac{\left[m_N V_{\rm S}^{[0]}(k;\Lambda)/(4\pi)\right]^{-1} + \mathcal{I}_{\rm L}^{[0]}(k;\Lambda)}{\chi_{\rm L}^{[0]}(\boldsymbol{p}',k;\Lambda)\,\chi_{\rm L}^{[0]}(\boldsymbol{p},k;\Lambda)}. \tag{55}$$

This is the generalization of Eq. (8) for LO in the presence of pions. Because $V_{\rm L}^{[0]}$ is regular, the cutoff dependence of the integrals $T_{\rm L}^{[0]}$ and $\chi_{\rm L}^{[0]}$ is only residual, i.e., suppressed by powers of Λ. In contrast, just as the $\mathcal{I}_0$ in Eq. (8), $\mathcal{I}_{\rm L}^{[0]}$ has a linear cutoff dependence due to the singularity of $V_{\rm S}^{[0]}$. Additionally, it exhibits a logarithmic dependence $\sim(m_\pi^2/M_{NN})\ln\Lambda$ [9] arising from the interference between $V_{\rm L}^{[0]}$ and $V_{\rm S}^{[0]}$. This cutoff dependence is at the root of one of the shortcomings of NDA in the NN system.

Compared to Refs. [9,26,54], our $V_{\rm S}^{[0]}$ has a different k dependence. As in the previous section, two dibaryon parameters are needed to describe the zero of the amplitude and its energy dependence near threshold, while the third parameter ensures the fine-tuning that leads to a large scattering length. These three parameters are sufficient for renormalization, leaving behind only residual cutoff dependence. Our LO amplitude is analogous to that of Ref. [37], which results from the unitarization of an expansion around the amplitude zero.

Taking the sharp-cutoff function $f_R(x) = \theta(1-x)$, we solve numerically the S-wave projection of Eq. (51), as done in, e.g., Refs. [26,49]. In order to determine the values of the three bare parameters at a given cutoff, three cutoff-independent conditions on the amplitude are needed. We choose them to be the same as in the previous section, i.e.,

(i) unitarity limit, $1/a^{[0]} = 0$;
(ii) physical effective range, $r_0 = 2.7$ fm;
(iii) physical amplitude zero, $k_0 = 340.4$ MeV.

The values of $\Delta_1^{[0]}(\Lambda)$, $\Delta_2^{[0]}(\Lambda)$, and $c_2^{[0]}(\Lambda)$ in our numerical calculations must be very well tuned in order to reproduce the required values of $1/a^{[0]}$, r_0, and k_0 within a given accuracy. The need for such a tuning becomes more and more noticeable as Λ is increased [49]. But the resulting phase shift changes dramatically depending on whether $1/a^{[0]}$ is very small and negative (for a shallow virtual state) or very small and positive (as it would correspond to a bound state close to threshold). Thus, in order to facilitate the numerical solution of the LS equation, we kept the scattering length large and negative, $a^{[0]} = -600$ fm. The difference with the unitarity limit cannot be seen in the results presented below.

The LO pionful phase shift is obtained from the on-shell, S-wave-projected T matrix in the usual way (21). The result, presented in Fig. 4, shows little cutoff dependence, even though the cutoff parameter is varied from 600 MeV to 2 GeV. It is likely that a more realistic estimate of the systematic error coming from the EFT truncation is obtained via the variation of the input inverse scattering length between its physical value and zero. We will come back to such an estimate later, when we resum finite-a effects. In any case, comparing with Fig. 2 we confirm that pions help us achieve a better description of phase shifts between threshold and the amplitude zero.

From the results in Fig. 4 we can obtain numerical predictions for parameters appearing in the ERE and in the expansion around the amplitude zero. As an example, we extract the LO shape parameter $P_0^{[0]}(\Lambda)$ using our low-energy results and the unitarity-limit version of the ERE (11) truncated at the level of the shape parameter. Results are shown in Fig. 5. For Λ large enough, we find

$$P_0^{[0]}(\Lambda) \approx P_0^{[0]}(\infty)\left(1 + \frac{Q_P}{\Lambda}\right), \tag{56}$$

with $P_0^{[0]}(\infty) \approx -1.0$ fm^3 and $Q_P \sim 100$ MeV. Unlike the result for the shape parameter given in Ref. [74], $P_0^{[0]}(\infty)$ is *negative*, being reasonably close to $P_0 = -1.9$ fm^3—the value extracted in Ref. [81] from the NijmII fit [70]. The large change

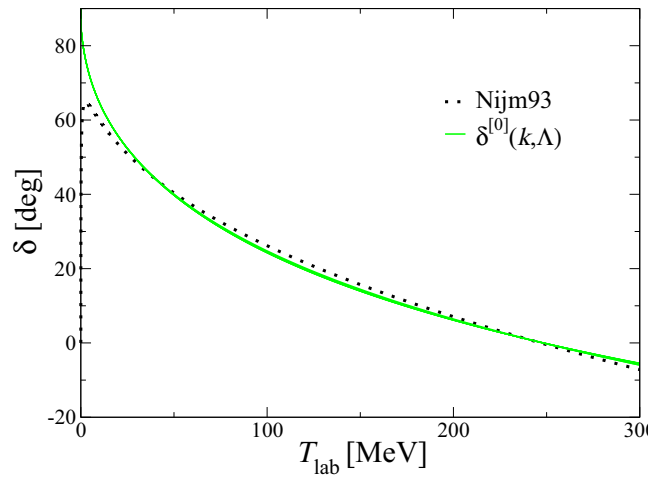

FIG. 4. np $^1S_0$ phase shift δ (in degrees) versus laboratory energy $T_{\rm lab} = 2k^2/m_N$ (in MeV) for χEFT at LO in our new PC. The narrow (green) band represents the evolution of the sharp cutoff from 600 MeV to 2 GeV. The (black) squares are the Nijm93 results [63,70].

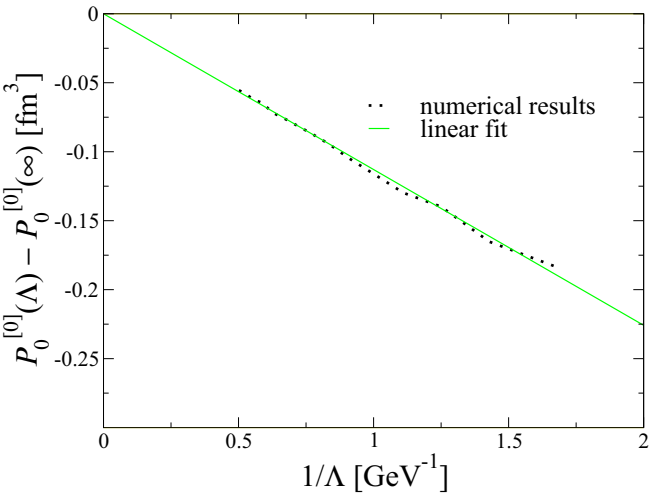

FIG. 5. np $^1S_0$ shape parameter $P_0^{[0]}(\Lambda)$ (in fm^3) versus inverse cutoff $1/\Lambda$ (in GeV^{-1}) for χEFT at LO in our new PC. The straight line represents a linear fit to the numerical values.

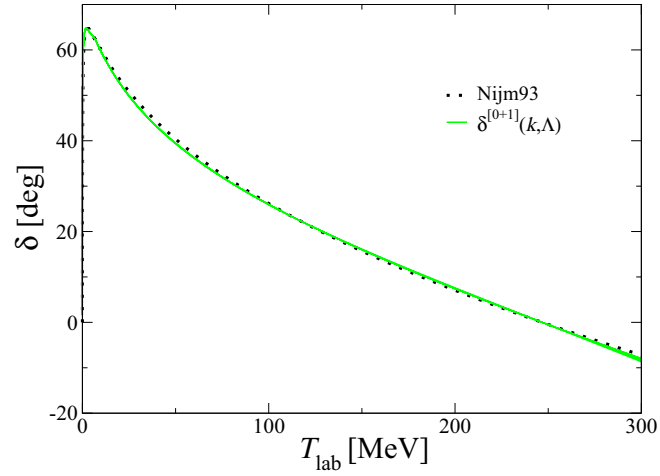

FIG. 6. np $^1S_0$ phase shift δ (in degrees) versus laboratory energy $T_{\rm lab} = 2k^2/m_N$ (in MeV) for χEFT at NLO in our new PC. The narrow (green) band represents the evolution of the cutoff from 600 MeV to 2 GeV. The (black) squares are the Nijm93 results [63,70].

in the prediction for $P_0^{[0]}(\infty)$ compared to the corresponding pionless result (29) is confirmation of the importance of pions at LO.

B. Next-to-leading order

As before, we can infer the short-range contributions at NLO from the residual cutoff dependence of the amplitude. Figure 5 shows that the cutoff dependence of $P_0^{[0]}(\Lambda)$ is proportional to $1/\Lambda$, with $Q_P = \mathcal{O}(M_{\rm lo})$ as expected. Just as in the pionless case, this behavior implies that at least one extra short-range parameter needs to be included at NLO. This is represented by the NLO potential $V^{[1]}$, Eq. (50).

Treating $V^{[1]}$ in distorted-wave perturbation theory, we obtain a separable NLO amplitude,

$$T^{[1]}(\boldsymbol{p}',\boldsymbol{p},k;\Lambda) = \chi^{[0]}(\boldsymbol{p}',k;\Lambda)\, V^{[1]}(k;\Lambda)\, \chi^{[0]}(\boldsymbol{p},k;\Lambda), \tag{57}$$

where

$$\chi^{[0]}(\boldsymbol{p},k;\Lambda) = 1 - m_N \int \frac{d^3q}{(2\pi)^3} \frac{f_R(q/\Lambda)}{q^2 - k^2 - i\epsilon}\, T^{[0]}(\boldsymbol{p},\boldsymbol{q},k;\Lambda), \tag{58}$$

is defined in terms of the *full* LO amplitude in analogy with Eq. (53) for the long-range LO amplitude. As in the pionless case, we obtain the pionful LO+NLO phase shift from Eq. (22).

The dibaryon parameters are fixed in virtue of four cutoff-independent conditions, which we choose to be the values of the Nijm93 phase shifts [63] at four different momenta:

(i) $\delta^{[0+1]}(20.0\ \text{MeV};\Lambda) = 61.1°$;
(ii) $\delta^{[0+1]}(40.5\ \text{MeV};\Lambda) = 64.5°$;
(iii) $\delta^{[0+1]}(237.4\ \text{MeV};\Lambda) = 21.7°$;
(iv) $\delta^{[0+1]}(340.4\ \text{MeV};\Lambda) = 0°$.

The LO+NLO phase shifts are shown in Fig. 6. The narrow band when the cutoff is varied from 600 MeV to 2 GeV confirms that, as in Fig. 4, very quick cutoff convergence takes place. The LO+NLO prediction almost lies on the Nijm93 curve, which means that now the description of the empirical phase shifts throughout the whole elastic range $0 \lesssim k \lesssim \sqrt{m_N m_\pi}$ is much better than at LO. Indeed, the improvement is clear not only in the very low momentum regime (which had been expected considering that now we relaxed the unitarity-limit condition) but—more importantly from the χEFT point of view—also for momenta $k \sim m_\pi$. Comparison with the pionless result at NLO (Fig. 3) confirms that adding OPE significantly improves predictions in this momentum range.

C. Resummation and higher orders

So far we took the binding momentum of the $^1S_0$ virtual state as an NLO parameter, since it is only about 6% of the pion mass and thus tiny on the scale of pion physics. We were guided by the PC presented in Sec. II, whose consistency could be demonstrated analytically. Despite the systematic improvement and good description of data at NLO, one might be distressed by the unusual appearance of our LO phase shift (Fig. 4) at low momentum. Within potential models—whether purely phenomenological or based on Weinberg's prescription—it is traditional to attempt to describe all regions below some arbitrary momentum on the same footing.

As emphasized earlier, plotting phase shifts is misleading when it comes to errors in the amplitude, which is the observable the PC is designed for. A plot of $k \cot\delta$ shows that only a small amount of physics is missed at LO even at low energies. Our strategy is a consequence of the fact that the PC assumes momenta $Q \sim M_{\rm lo}$, and it is in principle only in this region that we expect systematic improvement order by order. The higher the momentum, the smaller the relative

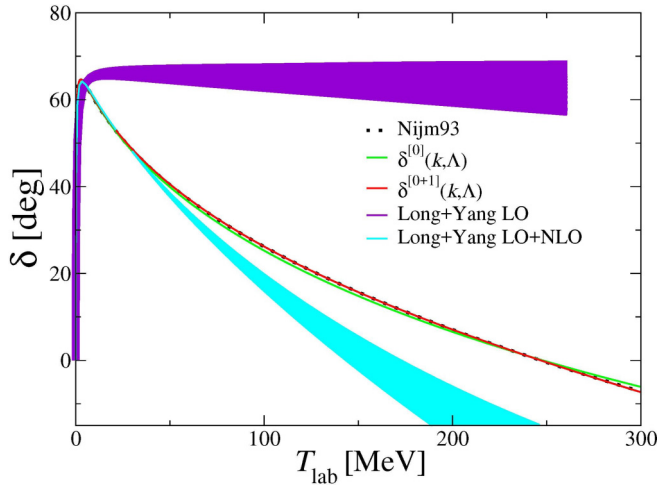

FIG. 7. np $^1S_0$ phase shift δ (in degrees) versus laboratory energy $T_{\rm lab} = 2k^2/m_N$ (in MeV) for χEFT at LO and NLO in our new PC from an alternative fitting protocol. The (green) light and (red) dark narrow bands represent, respectively, LO and LO+NLO under a cutoff variation from 600 MeV to 2 GeV. The LO and LO+NLO phase shifts from Ref. [26] have also been displayed; the upper (violet) LO band and the lower (cyan) LO+NLO band come from the same cutoff evolution as before. The (black) squares are the Nijm93 results [63,70].

improvement with order, until we reach $M_{\rm hi}$ and the EFT stops working. In the other direction, that of smaller momenta, the χEFT PC may no longer capture the relative importance of interactions properly. A simple example is pion-nucleon scattering in chiral perturbation theory, where sufficiently close to threshold the LO P-wave interaction [stemming from the axial-vector coupling in Eq. (46)] is smaller than NLO corrections to the S wave. Therefore the region of momenta much below the pion mass is *not* where one wants to judge the convergence of χEFT.

However, it might be of practical interest to improve the description near threshold already at LO. As in $\not\pi$EFT, we can choose to reproduce the empirical value of a phase shift in the very low-momentum region—thus accounting for nonvanishing $1/a$ already at LO—without doing damage to renormalization. As is the case with any other choice of data to fit, the difference with respect to what we have done earlier in this section is of NLO: We are just resumming some higher-order contributions into LO.

As an example, in Fig. 7 we show LO and LO+NLO results with an alternative fitting protocol. In the renormalization conditions at LO we replace the unitarity limit of our original fit with the physical scattering length, that is, we impose the following cutoff-independent conditions:

(i) $a = -23.7$ fm;
(ii) $r_0 = 2.7$ fm;
(iii) $k_0 = 340.4$ MeV.

Likewise, at NLO we substitute the lowest Nijm93 phase shift of our earlier fit with the physical scattering length:

(i) $a = -23.7$ fm;
(ii) $\delta^{[0+1]}(40.5\ {\rm MeV}) = 64.5^\circ$;
(iii) $\delta^{[0+1]}(237.4\ {\rm MeV}) = 21.7^\circ$;
(iv) $\delta^{[0+1]}(340.4\ {\rm MeV}) = 0^\circ$.

As before we vary the cutoff from 600 MeV to 2 GeV, but the Λ convergence of the phase shifts is so quick that the cutoff bands cannot be resolved in our plot. The improved description of the very low-energy region at LO compared to that seen in Fig. 4, which is entirely due to the resummation of the finite scattering length, is evident. The predicted LO+NLO phase shifts virtually lie on the Nijm93 curve, and this fit is even more phenomenologically successful than the original LO+NLO shown in Fig. 6. The relatively small improvement over the alternative LO curve is consequence of the resummation of higher-order contributions into LO. The small difference between alternative and original LO+NLO curves attests to the fine-tuning of the $^1S_0$ channel, i.e., to the smallness of $1/a$ effects.

The $^1S_0$ phase shifts resulting from the PC proposed by Long and Yang for the singlet waves [26] have also been plotted, at both LO and NLO, in Fig. 7. As mentioned before, the LO of such an arrangement—which, just like the LO of Weinberg's PC, consists of OPE supplemented by a short-range, momentum-independent term obtained through inputting the physical scattering length—manifestly fails in qualitatively reproducing the Nijm93 phase shift already at laboratory energies $T_{\rm lab} \gtrsim 20$ MeV, i.e., center-of-mass momenta $k \gtrsim 100$ MeV; in particular, the LO phase shift does not cross zero at any finite energy (when $\Lambda \gtrsim M_{\rm hi}$ [22]). In contrast, we see that, once the NLO interaction prescribed by Ref. [26]—the NLO correction to the LO counterterm, plus a two-derivative contact term determined by the empirical effective range—is added at first order in distorted-wave perturbation theory, the resulting phase shift turns out to have a zero at $T_{\rm lab} \sim 150$ MeV, i.e., $k \sim 250$ MeV or about 25% *below* its physical location k_0. Comparing the phase shifts at LO and NLO of Ref. [26] with the ones resulting from our new proposal, we confirm that, at the price of the inclusion of k_0 as an LO input and the promotion of $r_0(P_0)$ as a (N)LO input, the convergence of the new results is greatly improved.

Given the importance of OPE, one expects potentially large changes in the position of the poles of $T^{[0]}$ in χEFT with respect to the $\not\pi$EFT result (33). Yet, the virtual state near threshold (at $k \simeq i/a$) is guaranteed by construction, since

$$\frac{m_N}{4\pi} T^{[0]}(k;\Lambda) \overset{k\to 0}{\simeq} \left(\frac{1}{a} + ik\right)^{-1}. \tag{59}$$

Using the technique described in Ref. [49], one may obtain numerically the positions of the other two poles. The redundant pole seems to become deeper and deeper when the cutoff Λ is increased. This is consistent with the point of view that the redundant pole accounts in $\not\pi$EFT for the neglected left-hand cut due to OPE. In contrast, the binding energy of the deep bound state oscillates with Λ, but we always find it to be $\gtrsim 200$ MeV, which corresponds to a binding momentum $\gtrsim 450$ MeV. This is, again, an estimate for the breakdown scale $M_{\rm hi}$.

One might worry that the LO+NLO result shown in Fig. 7 is so good that higher orders could destroy agreement with the empirical phase shifts and undermine the consistency of our EFT expansion. At N^{2}LO and N^{3}LO there are several contributions to account for: TPE and the associated N^{2}LO counterterms [18,19] in first-order distorted-wave perturbation theory, as well as NLO interactions in second- and third-order distorted-wave perturbation theory. At these higher orders it might be convenient to use the perturbation techniques of Ref. [84] or to devise further resummation of NLO interactions.

To investigate the potential effects of higher-order corrections we have performed an incomplete N^{2}LO calculation where the long-range component of the N^{2}LO TPE potential was included in first-order distorted-wave perturbation theory, following the analogous calculation in Ref. [26]. Since the short-range component of this potential can be absorbed in Eq. (50), there are no new short-range parameters and we impose the same four renormalization conditions as in NLO. We have repeated the extraction of the phase shifts and found a negligible effect on the final result, so that this incomplete N^{2}LO phase shift is at least as good as the one plotted in Fig. 7. This indicates that in the $^1S_0$ channel the effects of the N^{2}LO TPE potential can be compensated by a change in the strengths of our LO and NLO short-range interactions. Of course, this is not a full calculation of the amplitude up to N^{2}LO, but since the change from LO to LO+NLO is small, we might expect the iteration of NLO interactions to also produce small effects. We intend to pursue full higher-order calculations in the future.

IV. CONCLUSIONS AND OUTLOOK

Despite its simplicity from the computational perspective, the two-nucleon $^1S_0$ channel has proven remarkably resistant to a systematic expansion. In this work we have developed a rearrangement of chiral EFT in this channel based on specific assumptions about the scaling of effective-range parameters and the amplitude zero with a single low-energy scale $M_{\rm lo} \sim 100$ MeV. Through the introduction of two dibaryon fields, we were able to reproduce empirical phase shifts very well already at NLO—that is, including interactions of up to relative $\mathcal{O}(M_{\rm lo}/M_{\rm hi})$—from threshold to beyond the zero of the amplitude at $k_0 \simeq 340$ MeV. The existence of a deep bound state at LO indicates that the expansion in powers of $M_{\rm lo}/M_{\rm hi}$ breaks down at a scale $M_{\rm hi} \sim 500$ MeV.

The new power counting is particularly transparent when pions are decoupled by an artificial decrease of their interaction strength, in which case a version of pionless EFT is produced. Even in this case LO and NLO fits to empirical phase shifts look reasonable, although the lack of pion exchange is noticeable in the form of the energy dependence.

The apparent convergence of our LO and NLO results towards the empirical phase shifts suggests that our PC might be the basis for a new chiral expansion in this channel. Our new expansion relies only on the identification of the *NN* amplitude zero as a low-energy scale, where the leading order of our EFT is expected to provide a qualitatively correct description of observables. Certainly there are other *NN* channels, such as $^3S_1$ and $^3P_0$, whose phase shifts cross zero at some point. However, the fact that both $^3S_1$ and $^3P_0$ channels are well described already at LO in a power counting consistent with renormalization invariance [10,22–25,27] suggests that the exact location of these zeros, unlike the one in $^1S_0$, can be reached by small, perturbative corrections. We have not investigated the consequences of adding multiple dimer fields in these waves. From our perspective, the $^1S_0$ channel is unique in having both a relatively low-energy zero and a fine-tuned S-matrix pole.

Before a claim of convergence in the $^1S_0$ channel can be made, however, one or two higher orders should be calculated, where additional long-range interactions appear in the form of multipion exchange. Indications already exist [22,26,54] that two-pion exchange and its counterterms, which enter first at N^{2}LO, are amenable to perturbation theory in this channel. However, it is yet to be checked whether their contributions are small enough not to destroy the excellent agreement obtained at NLO. This calculation is demanding because it requires treating the NLO interaction beyond first order in distorted-wave perturbation theory. An incomplete N^{2}LO calculation which omits these demanding terms suggests that higher orders might provide only very small corrections. We intend to consider also isospin-breaking corrections in the future, along the line of what was done in Ref. [66] for pionless EFT with unitarity at LO.

If this approach succeeds, then it raises new questions. For instance, can we find an equivalent momentum-dependent approach, which would be better suited to three-body calculations and beyond? If the answer is positive, then the idea of imposing the $^1S_0$ zero at leading order should be tested—together with consistent interactions in other channels which are order-by-order renormalizable—in future calculations of, e.g., few-body reactions or nuclear structure. Another important element that would demand an answer is the role of the quark masses in the power counting we propose here. We have worked at physical pion mass, but it remains to be seen how this new proposal can be implemented for arbitrary m_π in a renormalization-consistent manner. We intend to address these issues in future work.

ACKNOWLEDGMENTS

We thank J. A. Oller and M. Pavón Valderrama for useful discussions. U.v.K. is grateful to R. Higa, G. Rupak, and A. Vaghani for insightful comments on the role of low-energy amplitude zeros, which have inspired this manuscript. M.S.S. is grateful for hospitality to the Department of Physics at the University of Arizona, where part of this work was carried out. This research was supported in part by the National Natural Science Foundation of China (NSFC) through Grants No. 11375120, No. 11775148, and No. 11735003, by the U.S. Department of Energy, Office of Science, Office of Nuclear Physics, under Grant No. DE-FG02-04ER41338, and by the European Union Research and Innovation program Horizon 2020 under Grant No. 654002.

APPENDIX: RUNNING OF THE PIONLESS COUNTERTERMS

We collect in this Appendix the explicit cutoff dependence of the dibaryon couplings. These bare parameters ensure that the renormalization conditions in absence of long-range interactions, given by Eqs. (26) and (38) at LO and NLO, respectively, are fulfilled.

The bare parameters are given at LO by

$$\Delta_1^{[0]}(\Lambda) = \bar{\Delta}_1^{[0]} - \theta_1 \Lambda + \cdots , \tag{A1}$$

$$\frac{c_1^{[0]}(\Lambda)}{m_N} = 0, \tag{A2}$$

$$\Delta_2^{[0]}(\Lambda) = \frac{2\theta_1}{r_0^3 k_0^2}\left[\theta_1 (r_0\Lambda)^2 - \left(\frac{r_0^2 k_0^2}{2} + 2\theta_1\theta_{-1}\right) r_0\Lambda + 4\theta_1\theta_{-1}^2 + \cdots\right], \tag{A3}$$

$$\frac{c_2^{[0]}(\Lambda)}{m_N} = \frac{\bar{c}_2^{[0]}}{m_N} - \frac{2\theta_1}{r_0^3 k_0^4}\left[\theta_1 (r_0\Lambda)^2 - \left(r_0^2 k_0^2 + 2\theta_1\theta_{-1}\right) r_0\Lambda + 4\theta_1\theta_{-1}^2 + \cdots\right], \tag{A4}$$

and at NLO by

$$\Delta_1^{[1]}(\Lambda) = \bar{\Delta}_1^{[1]} + \cdots , \tag{A5}$$

$$\frac{c_1^{[1]}(\Lambda)}{m_N} = \frac{\bar{c}_1^{[1]}}{m_N} + \cdots , \tag{A6}$$

$$\begin{aligned}\Delta_2^{[1]}(\Lambda) = \bar{\Delta}_2^{[1]} &- \frac{\theta_1}{r_0^4} P_0^{[1]}(\Lambda)\left[\theta_1 (r_0\Lambda)^2 + \left(r_0^2 k_0^2 - 4\theta_1\theta_{-1}\right) r_0\Lambda - 2\theta_{-1}\left(r_0^2 k_0^2 - 6\theta_1\theta_{-1}\right)\right] \\ &- \frac{4\theta_1}{a r_0^2 k_0^2}(r_0\Lambda - 2\theta_{-1}) + \cdots ,\end{aligned} \tag{A7}$$

$$\frac{c_2^{[1]}(\Lambda)}{m_N} = \frac{\bar{c}_2^{[1]}}{m_N} + \frac{1}{k_0^2}\left(\bar{\Delta}_2^{[1]} - \Delta_2^{[1]}(\Lambda)\right) + \cdots . \tag{A8}$$

The "renormalized" couplings $(\bar{\Delta}_1^{[0]}, \ldots, \bar{c}_2^{[1]})$ are defined in the main text [see Eqs. (27) and (39)], and the ellipses account for terms that become arbitrarily small for an arbitrarily large cutoff.

[1] P. F. Bedaque and U. van Kolck, Ann. Rev. Nucl. Part. Sci. **52**, 339 (2002).
[2] E. Epelbaum, H.-W. Hammer, and U.-G. Meißner, Rev. Mod. Phys. **81**, 1773 (2009).
[3] D. R. Entem and R. Machleidt, Phys. Rept. **503**, 1 (2011).
[4] S. Weinberg, Phys. Lett. B **251**, 288 (1990).
[5] S. Weinberg, Nucl. Phys. B **363**, 3 (1991).
[6] M. Rho, Phys. Rev. Lett. **66**, 1275 (1991).
[7] A. Manohar and H. Georgi, Nucl. Phys. B **234**, 189 (1984).
[8] H. Georgi, Phys. Lett. B **298**, 187 (1993).
[9] D. B. Kaplan, M. J. Savage, and M. B. Wise, Nucl. Phys. B **478**, 629 (1996).
[10] A. Nogga, R. G. E. Timmermans, and U. van Kolck, Phys. Rev. C **72**, 054006 (2005).
[11] M. Pavón Valderrama and E. Ruiz Arriola, Phys. Rev. C **74**, 064004 (2006); **75**, 059905(E) (2007).
[12] C.-J. Yang, Ch. Elster, and D. R. Phillips, Phys. Rev. C **80**, 034002 (2009).
[13] C.-J. Yang, Ch. Elster, and D. R. Phillips, Phys. Rev. C **80**, 044002 (2009).
[14] Ch. Zeoli, R. Machleidt, and D. R. Entem, Few-Body Syst. **54**, 2191 (2013).
[15] M. P. Valderrama and D. R. Phillips, Phys. Rev. Lett. **114**, 082502 (2015).
[16] D. B. Kaplan, M. J. Savage, and M. B. Wise, Phys. Lett. B **424**, 390 (1998).
[17] D. B. Kaplan, M. J. Savage, and M. B. Wise, Nucl. Phys. B **534**, 329 (1998).
[18] C. Ordóñez and U. van Kolck, Phys. Lett. B **291**, 459 (1992).
[19] C. Ordóñez, L. Ray, and U. van Kolck, Phys. Rev. C **53**, 2086 (1996).
[20] S. Fleming, T. Mehen, and I. W. Stewart, Nucl. Phys. A **677**, 313 (2000).
[21] M. C. Birse, Phys. Rev. C **74**, 014003 (2006).
[22] M. Pavón Valderrama, Phys. Rev. C **83**, 024003 (2011).
[23] M. Pavón Valderrama, Phys. Rev. C **84**, 064002 (2011).
[24] B. Long and C.-J. Yang, Phys. Rev. C **84**, 057001 (2011).
[25] B. Long and C.-J. Yang, Phys. Rev. C **85**, 034002 (2012).
[26] B. Long and C.-J. Yang, Phys. Rev. C **86**, 024001 (2012).
[27] Y.-H. Song, R. Lazauskas, and U. van Kolck, Phys. Rev. C **96**, 024002 (2017).
[28] M. P. Valderrama, M. S. Sánchez, C.-J. Yang, B. Long, J. Carbonell, and U. van Kolck, Phys. Rev. C **95**, 054001 (2017).
[29] D. B. Kaplan, Nucl. Phys. B **494**, 471 (1997).

[30] T. D. Cohen and J. M. Hansen, Phys. Lett. B **440**, 233 (1998).
[31] J. V. Steele and R. J. Furnstahl, Nucl. Phys. A **645**, 439 (1999).
[32] T. Mehen and I. W. Stewart, Phys. Rev. C **59**, 2365 (1999).
[33] T. Frederico, V. S. Timóteo, and L. Tomio, Nucl. Phys. A **653**, 209 (1999).
[34] J. Gegelia, Phys. Lett. B **463**, 133 (1999).
[35] D. B. Kaplan and J. V. Steele, Phys. Rev. C **60**, 064002 (1999).
[36] C. H. Hyun, D.-P. Min, and T.-S. Park, Phys. Lett. B **473**, 6 (2000).
[37] M. Lutz, Nucl. Phys. A **677**, 241 (2000).
[38] S. R. Beane, P. F. Bedaque, M. J. Savage, and U. van Kolck, Nucl. Phys. A **700**, 377 (2002).
[39] J. M. Nieves, Phys. Lett. B **568**, 109 (2003).
[40] J. A. Oller, Nucl. Phys. A **725**, 85 (2003).
[41] M. Pavón Valderrama and E. Ruiz Arriola, Phys. Lett. B **580**, 149 (2004).
[42] M. P. Valderrama and E. R. Arriola, Phys. Rev. C **70**, 044006 (2004).
[43] V. S. Timóteo, T. Frederico, A. Delfino, and L. Tomio, Phys. Lett. B **621**, 109 (2005).
[44] M. Pavón Valderrama and E. Ruiz Arriola, Phys. Rev. C **74**, 054001 (2006).
[45] J.-F. Yang and J.-H. Huang, Commun. Theor. Phys. **47**, 699 (2007).
[46] D. R. Entem, E. Ruiz Arriola, M. Pavón Valderrama, and R. Machleidt, Phys. Rev. C **77**, 044006 (2008).
[47] J. Soto and J. Tarrús, Phys. Rev. C **78**, 024003 (2008).
[48] D. Shukla, D. R. Phillips, and E. Mortenson, J. Phys. G **35**, 115009 (2008).
[49] C.-J. Yang, Ch. Elster, and D. R. Phillips, Phys. Rev. C **77**, 014002 (2008).
[50] M. C. Birse, Eur. Phys. J. A **46**, 231 (2010).
[51] K. Harada, H. Kubo, and Y. Yamamoto, Phys. Rev. C **83**, 034002 (2011).
[52] S.-I. Ando and C. H. Hyun, Phys. Rev. C **86**, 024002 (2012).
[53] S. Szpigel and V. S. Timóteo, J. Phys. G **39**, 105102 (2012).
[54] B. Long, Phys. Rev. C **88**, 014002 (2013).
[55] K. Harada, H. Kubo, T. Sakaeda, and Y. Yamamoto, arXiv:1311.3063 [nucl-th].
[56] E. Epelbaum, A. M. Gasparyan, J. Gegelia, and H. Krebs, Eur. Phys. J. A **51**, 71 (2015).
[57] X.-L. Ren, K.-W. Li, L.-S. Geng, B.-W. Long, P. Ring, and J. Meng, Chinese Phys. C **42**, 014103 (2018).
[58] B. Long, Int. J. Mod. Phys. E **25**, 1641006 (2016).
[59] M. Pavón Valderrama, Int. J. Mod. Phys. E **25**, 1641007 (2016).
[60] U. van Kolck, Lect. Notes Phys. **513**, 62 (1998).
[61] U. van Kolck, Nucl. Phys. A **645**, 273 (1999).
[62] V. G. J. Stoks, R. A. M. Klomp, M. C. M. Rentmeester, and J. J. de Swart, Phys. Rev. C **48**, 792 (1993).
[63] NN-OnLine http://nn-online.org/.
[64] S. R. Beane and M. J. Savage, Nucl. Phys. A **694**, 511 (2001).
[65] A. Vaghani, R. Higa, G. Rupak, and U. van Kolck (unpublished).
[66] S. König, H. W. Grießhammer, H.-W. Hammer, and U. van Kolck, J. Phys. G **43**, 055106 (2016).
[67] L. Castillejo, R. H. Dalitz, and F. J. Dyson, Phys. Rev. **101**, 453 (1956).
[68] D. R. Entem and J. A. Oller, Phys. Lett. B **773**, 498 (2017).
[69] M. I. Krivoruchenko, Phys. Rev. C **82**, 018201 (2010).
[70] V. G. J. Stoks, R. A. M. Klomp, C. P. F. Terheggen, and J. J. de Swart, Phys. Rev. C **49**, 2950 (1994).
[71] H. W. Grießhammer, Nucl. Phys. A **744**, 192 (2004).
[72] L. Koester and W. Nistler, Z. Physik **272**, 189 (1975).
[73] E. Lomon and R. Wilson, Phys. Rev. C **9**, 1329 (1974).
[74] V. A. Babenko and N. M. Petrov, Phys. Atom. Nucl. **73**, 1499 (2010).
[75] P. F. Bedaque, H.-W. Hammer, and U. van Kolck, Nucl. Phys. A **676**, 357 (2000).
[76] L. Platter, H.-W. Hammer, and U.-G. Meißner, Phys. Lett. B **607**, 254 (2005).
[77] I. Stetcu, B. R. Barrett, and U. van Kolck, Phys. Lett. B **653**, 358 (2007).
[78] L. Contessi, A. Lovato, F. Pederiva, A. Roggero, J. Kirscher, and U. van Kolck, Phys. Lett. B **772**, 839 (2017).
[79] S. König, H. W. Grießhammer, H.-W. Hammer, and U. van Kolck, Phys. Rev. Lett. **118**, 202501 (2017).
[80] W. T. H. van Oers and J. D. Seagrave, Phys. Lett. B **24**, 562 (1967).
[81] M. Pavón Valderrama and E. Ruiz Arriola, arXiv:nucl-th/0407113.
[82] S. T. Ma, Phys. Rev. **69**, 668 (1946).
[83] S. T. Ma, Phys. Rev. **71**, 195 (1947).
[84] J. Vanasse, Phys. Rev. C **88**, 044001 (2013).